

The Interstellar Boundary Explorer (IBEX): Tracing the Interaction between the Heliosphere and Surrounding Interstellar Material with Energetic Neutral Atoms

Priscilla C. Frisch · David J. McComas

Accepted

Abstract The Interstellar Boundary Explorer (IBEX) mission is exploring the frontiers of the heliosphere where energetic neutral atoms (ENAs) are formed from charge exchange between interstellar neutral hydrogen atoms and solar wind ions and pickup ions. The geography of this frontier is dominated by an unexpected nearly complete arc of ENA emission, now known as the IBEX 'Ribbon'. While there is no consensus agreement on the Ribbon formation mechanism, it seems certain this feature is seen for sightlines that are perpendicular to the interstellar magnetic field as it drapes over the heliosphere. At the lowest energies, IBEX also measures the flow of interstellar H, He, and O atoms through the inner heliosphere. The asymmetric oxygen profile suggests that a secondary flow of oxygen is present, such as would be expected if some fraction of oxygen is lost through charge exchange in the heliosheath regions. The detailed spectra characterized by the ENAs provide time-tagged samples of the energy distributions of the underlying ion distributions, and provide a wealth of information about the outer heliosphere regions, and beyond.

Keywords Energetic neutral atoms · Heliosphere · Solar wind · ISM: atoms · ISM: magnetic fields · ISM: kinematics and dynamics · Interplanetary medium

1 Introduction

The newest frontier in space exploration is close to home, where the outflowing magnetized solar wind plasma meets and mixes with the interstellar cloud at the heliosphere's boundaries. The evolving heliosphere is formed by the relative ram (dynamic) pressures of the solar wind and partially ionized low density, $\sim 0.3 \text{ cm}^{-3}$, interstellar cloud flowing around (interstellar ions and magnetic field) and through (interstellar neutrals) the heliosphere at 26.3 km s^{-1} . The interstellar neutrals dominate the mass-density in the heliosphere beyond

P. C. Frisch
University of Chicago Dept. Astronomy and Astrophysics, Chicago, Illinois
Tel.: 773-702-0181
Fax: 773-702-8212
E-mail: frisch@oddjob.uchicago.edu

D. J. McComas
Southwest Research Research Institute and University of Texas, San Antonio, Texas

10–15 AU, and are able to penetrate deep into the inner heliosphere. Gravitational focusing of heavy elements in the flow forms the helium focusing cone that the Earth traverses early every December. The Interstellar Boundary Explorer (IBEX) mission (McComas et al. 2009b) has recently mapped the energetic neutral atoms (ENAs) that are formed by charge-exchange between heliosphere plasmas and interstellar neutrals in the heliosheath regions. These maps are now reshaping our understanding of the heliospheric interaction with the interstellar medium. IBEX has also made the first *in situ* detection of the flow of interstellar oxygen through the heliosphere (Möbius et al. 2009).

The presence of interstellar neutrals in the heliosphere was established 40 years ago. OGO 5 mapped the H° Lyman alpha sky background and showed a diffuse component attributed to interstellar neutral hydrogen in the inner heliosphere (Thomas and Krassa 1971; Bertaux and Blamont 1971). A *Copernicus* spectrum of this weak $\text{Ly}-\alpha$ emission firmly established it as interstellar (Adams and Frisch 1977). Measurements of the fluorescence of solar 584 Å emission from interstellar He° in the heliosphere revealed the helium focusing cone (Weller and Meier 1974). The discovery of helium pickup ions (Möbius et al. 1985) showed that the ionization of interstellar neutrals inside of the heliosphere produces energetic ions that trace the neutrality of the interstellar cloud around the Sun. Inside of the heliosphere, interstellar neutrals are ionized through charge-exchange with the solar wind, photoionization, and for those neutrals surviving to 1 AU electron-impacts (Rucinski et al. 1996). Pickup ions are a crucial diagnostic of the interaction between the heliosphere and the interstellar medium.

ENAs formed from charge-exchange between interstellar neutrals and solar wind ions were recognized as an important remote diagnostic of the distant heliosphere boundary regions (Gruntman 1993; Hsieh and Gruntman 1993). ENAs with energies 55–80 keV, originating in the heliosheath, were discovered by CELIAS/HSTOF on SOHO (Hilchenbach et al. 1998). IBEX maps of ENAs produced in the heliosphere boundaries, and the unexpected discovery of the IBEX Ribbon, requires a new paradigm for understanding the interaction between the heliosphere and interstellar medium (McComas et al. 2009a; Funsten et al. 2009a; Fuselier et al. 2009b; Schwadron et al. 2009).

Interstellar neutral helium is the best marker for the upwind direction of the ISM flowing through the heliosphere, usually denoted the heliosphere nose direction. Möbius et al. (2004) combined several data sets to obtain an upwind direction toward $\lambda, \beta \sim 255^\circ, 5^\circ$ (or in galactic coordinates, $\ell \sim 4^\circ, b \sim 15^\circ$). Photoionization models of the interstellar cloud surrounding the heliosphere, that are constrained by the observed properties of interstellar material inside and surrounding the heliosphere, show that the circumheliospheric interstellar cloud is low density, partially ionized, and warm, $n(\text{H}^\circ) \sim 0.20 \text{ cm}^{-3}$, $n(\text{e}^-) \sim 0.07 \text{ cm}^{-3}$, $n(\text{p}^+) \sim 0.06 \text{ cm}^{-3}$, and $T \sim 6300 \text{ K}$ (Model 26 in Slavin and Frisch 2008). If thermal and magnetic pressures are similar, the interstellar magnetic field (ISMF) strength is $\sim 2.7 \mu\text{G}$.

2 Measurements of Energetic Neutral Atoms from the Heliosphere Boundaries

IBEX was launched October 19, 2008 into low-Earth orbit and subsequently raised itself into a highly ecliptical orbit, $\sim 2 - 50 R_{\text{Earth}}$. The IBEX spacecraft is Sun-pointing, and spins four times a minute, so that the two oppositely mounted detectors, IBEX-Hi (Funsten et al. 2009b) and IBEX-Lo (Fuselier et al. 2009a) measure ENAs over great circle swaths of the sky. The spacecraft is repointed towards the Sun once a week, yielding an effective angular resolution of $\sim 7^\circ$ in longitude. IBEX completes two all-sky ENA maps per year. The first set of sky maps were collected December 2008 through June 2009 (McComas et al. 2009a) and

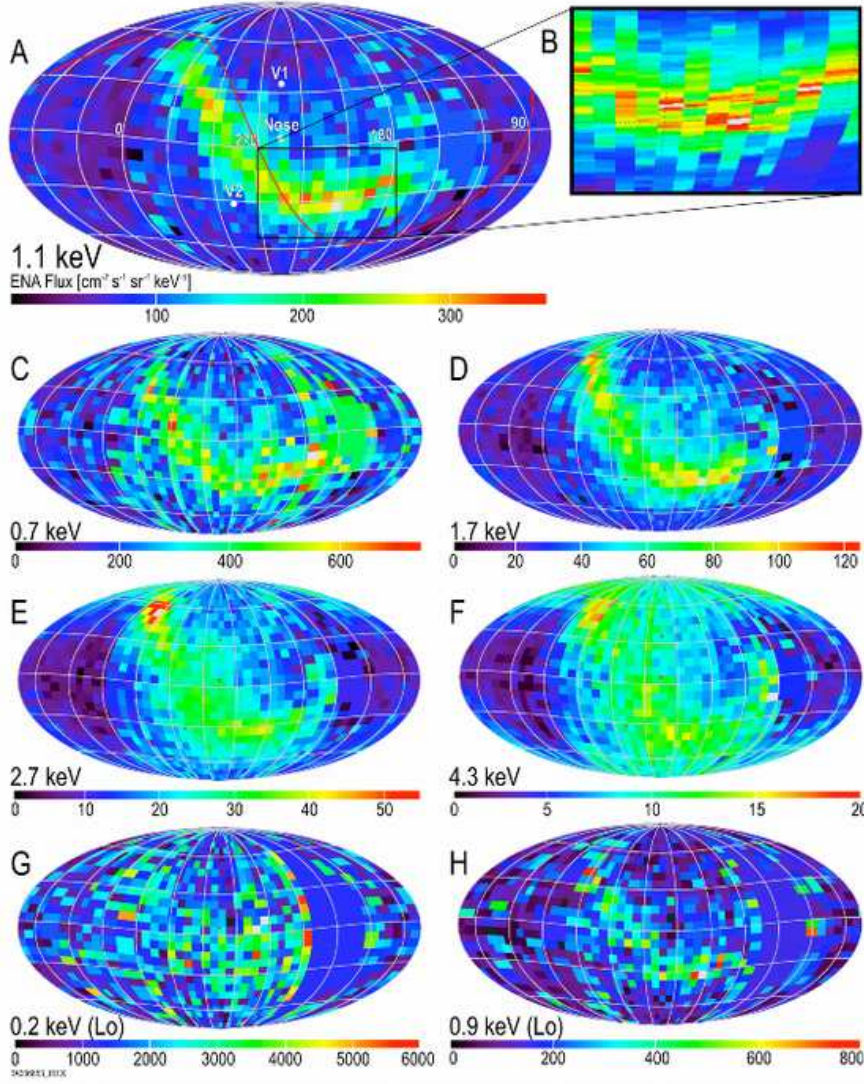


Fig. 1 IBEX measurements of the first all-sky maps of ENA fluxes over central energies of 0.2 keV (Lo) through 4.3 keV (Hi). The maps are Mollweide projections in ecliptic coordinates (J2000), and are centered near the longitude of the heliosphere nose. Also shown are the galactic plane (red line in upper figure) and the current locations of the Voyager 1 (at $\lambda, \beta = 255^\circ, 34^\circ$) and Voyager 2 ($289^\circ, -29^\circ$) satellites. The prominent arc of bright emission is the IBEX Ribbon. The Ribbon is not ordered by either ecliptic or galactic coordinates, but instead appears to form where the sightlines are perpendicular to the direction of the interstellar magnetic field draping over the heliosphere. The magnified region shows fine scale structure in the Ribbon, which has been identified by smoothing each 0.5° angle in spin phase along a measurement swath by the amount needed to reach 10% counting statistics. The ENA energies are plotted in the spacecraft frame. Pixels in the small area near $\lambda \sim 120^\circ - 150^\circ$ are contaminated by the magnetosphere, and are filled in by extrapolation from adjacent regions. (The figure is from McComas et al. 2010).

the second set from June through December 2009 (McComas et al. 2010), during periods when the orbit apogee was primarily outside of the magnetosphere and in the magnetosheath and solar wind. IBEX-Lo has eight energy channels that measure ENAs in the interval $\sim 0.01 - 2$ keV. IBEX-Lo also has the capability to directly measure the impact of neutral atoms with relatively high densities in the surrounding interstellar cloud, such as H, He, O, and possibly Ne, during certain portions of the yearly orbit (Möbius et al. 2009). IBEX-Hi has six energy channels covering $\sim 0.3 - 6$ keV.

2.1 Characteristics of the ENA Sky

The IBEX all-sky maps of ENA fluxes for IBEX-Hi and IBEX-Lo energy bands are shown in Figure 1, in units of $\text{cm}^{-2} \text{s}^{-1} \text{sr}^{-1} \text{keV}^{-1}$. These maps are centered near the heliosphere nose, located at ecliptic coordinates $\lambda \sim 255^\circ$, $\beta \sim 5^\circ$. The distribution of ENA emission on the sky is not ordered by either ecliptic or galactic coordinates. The most obvious feature in the ENA sky is the newly-discovered bright 'Ribbon' of ENA emission. The Ribbon forms a nearly complete arc on the sky, centered $\sim 46^\circ$ from the heliosphere nose toward λ , $\beta \sim 221^\circ$, 39° . None of the pre-launch ENA models predicted the Ribbon.

The IBEX Ribbon is observed between 0.2 and 6 keV, with an average width that is independent of energy and narrow ($\sim 20^\circ$, Fuselier et al. 2009b). The Ribbon width is determined by averaging ENA fluxes over 60° segments across the Ribbon, and normalizing the co-added segments by fitting and subtracting the underlying distributed emission (Figure 2). The excess emissions in both figures for angles to the Ribbon-center line of $\sim 12 - 30^\circ$ are counts from directly detected interstellar neutrals (Section 3). The Ribbon is therefore

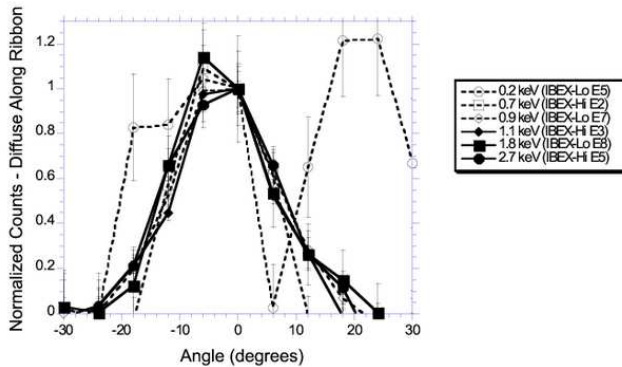


Fig. 2 Energy fluxes shown for a cut across the IBEX Ribbon in directions that are approximately perpendicular to the arc of the Ribbon. The Ribbon fluxes are normalized by a baseline distributed emission that is subtracted at each energy, where the baseline flux is a linear polynomial that is required to fit the total ENA fluxes well outside of the Ribbon arc. After normalizing the Ribbon fluxes by the relatively smooth distributed emission, the full-width-half-max of the Ribbon is $\sim 20^\circ$ at each of the IBEX energy bands where the Ribbon is apparent (0.1 keV – 6 keV), with the exception of the 1.1 keV channel where fluxes are enhanced at the core solar wind energy. The Ribbon fluxes are 2–3 times the fluxes of the distributed emissions. (This figure is from Fuselier et al. 2009b).

characterized as a coherent long and narrow arc in the sky, spanning $\geq 300^\circ$, with a similar spatial morphology over the IBEX energy range.

The Ribbon contains fine structure, including small regions of bright ENA emission, or ‘hot-spots’, that are several pixels wide and of different lengths (McComas et al. 2009a). The most prominent hot-spot, referred to as the “knot” in the ribbon, is located near $\lambda \sim 350^\circ$, $\beta \sim 60^\circ$. The second all-sky map has shown that this knot diminished and spread out along the Ribbon over the six months between the first and second set of skymaps (McComas et al. 2010).

The ages of the ENAs forming a skymap vary because of the energy-dependent time-lag between the creation of the solar wind (SW) ion that nucleates the ENA, and the ENA detection by IBEX. Also, a single skymap is collected over six months. The round trip ENA travel time to the termination shock, nominally at ~ 100 AU, is 4.3–1.3 years for IBEX-Hi ESA2 and ESA6 (when the entire energy channel widths are included). ENAs originating near the heliopause (~ 160 AU in the upwind direction), show even larger possible time-lags of 6.8 – 2.0 year for round trip travel times.

These travel time-lags suggest that the heliosheath ENAs contributing to the first skymaps were produced partly by solar wind emitted during the extreme solar minimum conditions of the declining phase of the Solar Cycle 23. The solar wind varies between solar minimum with typical velocities ~ 400 km s $^{-1}$, to solar maximum with velocities ~ 500 km s $^{-1}$ or more. Therefore tracking the observed ENAs back to the parent ions will require folding the solar-cycle dependence of the heliosphere into detailed models for ENA production as a function of energy and location.

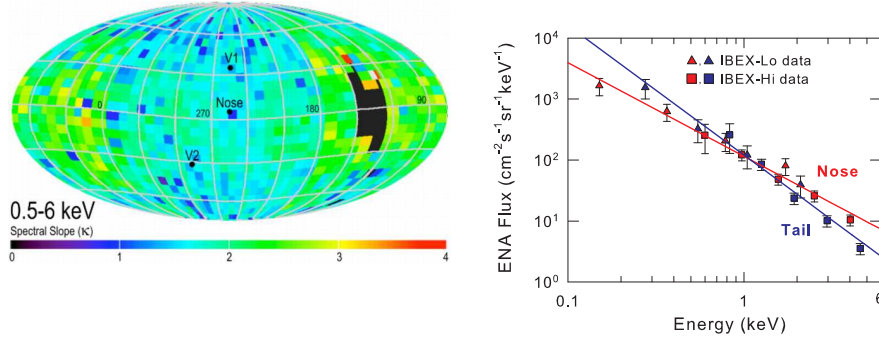


Fig. 3 Left: Skymap of the power law slope of the ENA spectrum, κ , over the sky for ENA energies 0.5–6 keV using IBEX-Hi data (from McComas et al. 2009a). The region contaminated by the magnetosphere is left black here. Right: The power law slope of the ENA spectrum in the direction of the heliosphere nose region (red) and tail region (blue). Note the softer spectrum towards the tail (from Funsten et al. 2009a).

2.2 Energy Distributions of IBEX ENAs

Fits to nine energy channels 0.7–6 keV show that the ENA spectra generally follow the power laws that characterize the energy distribution of the underlying non-thermal heliosheath plasmas (McComas et al. 2009a; Funsten et al. 2009a). The spectral index of ENA emission can be described by a kappa distribution, consisting of a thermal core and power-law with

exponent κ at high energies (Vasyliunas 1968). ENA spectra vary with ecliptic longitude and latitude for energies > 0.5 keV (Figure 3). Outside of the Ribbon, the globally distributed flux in the north and south polar regions ($\beta > |54^\circ$) have more complicated spectral shapes that can not be fit with a single kappa distribution. For the low latitude spectra, including both the distributed and Ribbon emission, a power law of $\kappa = 1.5$ is seen towards the nose regions, with a softer spectra $\kappa = 2.1$ in the direction of the elongated tail. The harder ENA spectra near the polar regions may result from increased solar wind velocities at high latitudes. The softer tail ENA spectrum may show the slowdown of the solar wind in the tail because of energy loss by charge-exchange with interstellar neutrals. For a constant ENA production rate as a function of energy and distance, the differential cross-sections would lead to a hardening of the ENA spectra with the distance of the formation region. The charge-exchange cross sections decrease with increasing energy (Lindsay and Stebbings 2005), for example varying by a factor of ~ 2 between 0.5 keV (the FWHM lower energy of IBEX-Hi ESA2) and 6.0 keV (the FWHM upper energy of IBEX-Hi ESA6).

Surprisingly, the Ribbon does not create an obvious feature in the ENA energy distribution, even though the fluxes are several times larger than for adjacent regions. The spectra of the Ribbon is characterized by several κ values. There is a slight tendency for κ to be slightly softer, ~ 0.3 , in the low-latitude Ribbon emission than in the low-latitude distributed emission (Figure 2A and 2B in Funsten et al. 2009a). The Ribbon spectra at high-latitude is similar to the spectra of the distributed emission, with the exception of the bright emission knot. At 1.7 and 2.7 keV the knot flux is highly variable over small spatial scales and shows enhanced fluxes compared to the distributed emission. This emission knot is located toward a region where slow and fast solar winds may interact, suggesting possible unusual conditions for energizing the pickup ions for such a termination shock location (McComas et al. 2009a). The second IBEX sky maps show that the knot emission is time-variable (McComas et al. 2010).

3 Measuring the Flow of Interstellar Neutrals through the Inner Heliosphere

IBEX-Lo has the capability to expand the sample of cosmic material that has been detected in situ by spacecraft, and provide volume densities for key interstellar elements. Several elements in the circumheliospheric interstellar material (ISM) have a significant fraction of interstellar neutrals (ISNs), such as H ($\sim 78\%$), He ($\sim 61\%$), O ($\sim 81\%$) and Ne ($\sim 20\%$, Model 26 in Slavin and Frisch 2008). Hydrogen and oxygen have similar first ionization potentials and are tightly coupled in the local ISM. The volume densities of ISNs inside of the heliosphere are related to the ionization state of the circumheliospheric ISM, once filtration in the heliosheath regions is included. Volume densities are difficult to obtain astronomically in general, and almost impossible to obtain for low density clouds such as the one that surrounds the Sun, making the IBEX-Lo measurements a valuable diagnostic of the ionization level and physical properties of the surrounding ISM.

The ISNs enter the heliosphere at interstellar velocities (~ 26.3 km s $^{-1}$) and follow Keplerian orbits modified by gravity and radiation pressure into the inner heliosphere. IBEX-Lo includes the capability to directly image the flow of several interstellar neutrals during parts of the year where gravitational deflection and orbital motions boost neutral velocities above the IBEX-Lo detection threshold of 0.01 keV. These directly detected ISNs create peaks in count rates in the IBEX-Lo sky-maps, at element-specific orbits where the required energy boost is sufficient (e.g. Figure 1 in Möbius et al. 2009). Interstellar H and He create pronounced features in the IBEX-Lo maps at 0.015 keV and 0.11 keV, and the weaker O

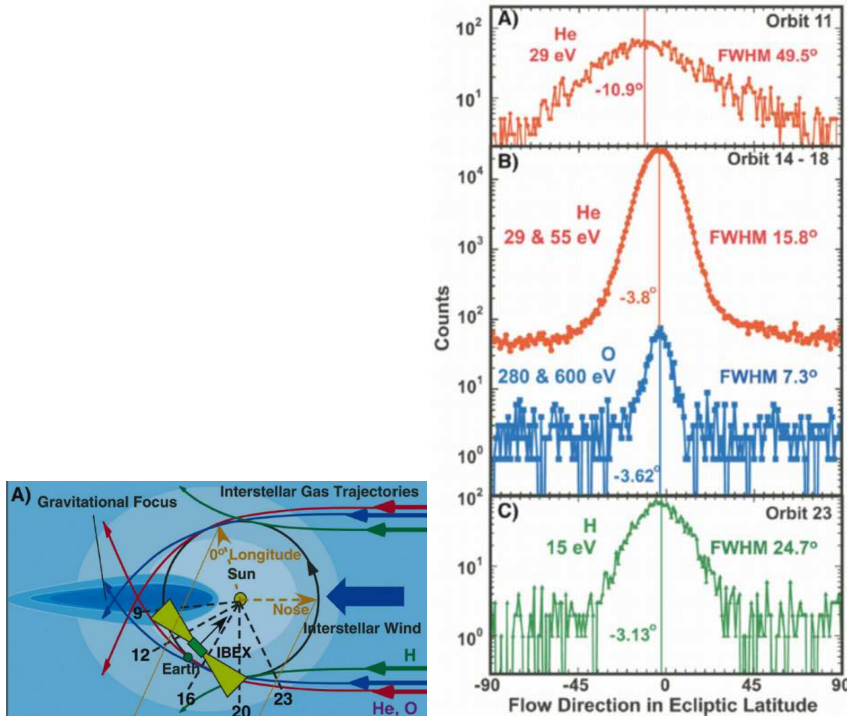


Fig. 4 Left: Cartoon showing the flow of interstellar neutrals through the inner heliosphere as deflected by gravity. The He focusing cone is shown in blue. Gravitational deflections are stronger for lighter atoms (He, red) than heavier atoms (O, blue), so that they are detected during different parts of the orbit. Hydrogen atoms are deflected by radiation pressure (green). The Earth's positions during IBEX orbits 9–23 is shown, along with the IBEX FOV for orbit 14. Right: Direct measurements by IBEX-Lo of the flow of interstellar H (C), He (A and B), and O (B) are shown as a function of the ecliptic latitude. The central and FWHM of each distribution were found from Gaussian fits to the incoming flow, convoluted with the IBEX-Lo angular response function. Counts are integrated over 1° bins. (These figures are from Möbius et al. 2009).

enhancement is visible at 0.6 keV. All three neutrals arrive from a direction that appears consistent with the inflowing He° direction measured by Ulysses (Möbius et al. 2004), slightly above the ecliptic plane. The IBEX scan strategy gives the distribution of interstellar H° , He° , and O° as a function of ecliptic latitude (Figure 4). The ISN particle trajectories are reconstructed using a hot-model of the ISM flow, incident velocities of 26.3 km s^{-1} , and ISN gas temperatures of 6,300 K. The oxygen latitudinal distribution shows an asymmetry, with a weak enhancement down to $\beta \sim -30^\circ$, that suggests that a secondary component of the interstellar O flow forms from the ionized O that is deflected around the heliopause together with the deflected hydrogen. A secondary He component is possible (Möbius et al. 2009, private communication).

4 Whence the ENA Ribbon?

IBEX's discovery of a Ribbon of ENA emission was entirely unexpected, but at the same time the fundamental directions traced by the Ribbon are consistent with pre-launch MHD

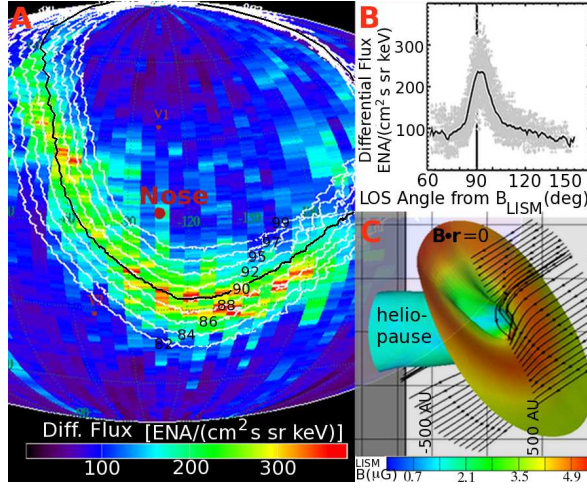


Fig. 5 (A) The contours of $B \cdot R$ predicted by MHD models of the heliosphere (Schwadron et al. 2009; Pogorelov et al. 2009) are superimposed on the 1 keV ENA map. The black contour shows $B \cdot R \sim 0$, where the ISMF is perpendicular to the sightline R . The contour labels give the angle between the sightline and B_{LISM} . (B) Plot of the differential ENA flux at 1 keV versus the $B \cdot R$ angle, with the Ribbon emission peak at an angle of 90° clearly visible. (C) The global configuration of the ISMF field lines draped over the heliosphere, and the surface where $B \cdot R \sim 0$ (red), and is the 3D realization of the black contour in (A) (figure from Schwadron et al. 2009).

heliosphere models that reproduce known asymmetries (Schwadron et al. 2009; Pogorelov et al. 2009). The asymmetries include the 10 AU difference between termination shock encounters by Voyager 1 (34° above the ecliptic plane, Figure 1) and Voyager 2 (29° below the plane), the 5° offset between the inflow directions of interstellar H° and He° into the heliosphere (after correction to J2000 coordinates, Lallement et al. 2005; Frisch 2010), and the distribution along the galactic plane of 3 kHz emissions detected by the Voyager satellites during the early 1990's (Kurth and Gurnett 2003). The observed asymmetries impose the restriction that the direction of the interstellar magnetic field is near the plane formed by inflowing H° and He° velocity vectors, the 'hydrogen deflection plane', and that it makes some angle, e.g. $\sim 45^\circ$, with the gaseous flow velocity (Pogorelov et al. 2009; Opher et al. 2009). Figure 5 (A) compares the 1 keV Ribbon fluxes with $B \cdot R \sim 0$ (from the MHD heliosphere model of Pogorelov et al. 2009) which includes ion-neutral coupling with a kinetic description of the neutrals and Lorentzian description of the ions. A plot of the fluxes versus $B \cdot R$ is shown in (B), while (C) shows a 3D figure of the ISMF lines draping over the heliosphere, together with the $B \cdot R = 0$ surface. The ISMF-driven asymmetry is offset by the symmetrizing effect of charge-exchange with the partially ionized low density cloud around the Sun ($n(\text{H}^\circ) \sim 0.2 \text{ cm}^{-3}$, $n(\text{H}^+) \sim 0.07 \text{ cm}^{-3}$, $T \sim 6,300 \text{ K}$). Remarkably, the centroid ridge of the IBEX Ribbon was found to track directions where the Pogorelov et al. heliosphere model indicates that the ISMF draping over the heliosphere is perpendicular to the sightline (Figure 5, A). The central direction of the Ribbon arc, towards galactic coordinates $L, B = 33^\circ, 55^\circ$ (or ecliptic coordinates $\lambda, \beta = 221^\circ, 39^\circ$, Funsten et al. 2009a) is within the $\pm 35^\circ$ uncertainties of the best fitting local ISM magnetic field direction of $L, B = 38^\circ, 23^\circ$, found from starlight polarizations caused by magnetically aligned interstellar dust grains (Frisch et al. 2010b). The discovery of the IBEX Ribbon requires rethinking our paradigm

of how the solar wind interacts with interstellar gas in the surrounding cloud, a process that fundamentally determines the characteristics of the heliosphere.

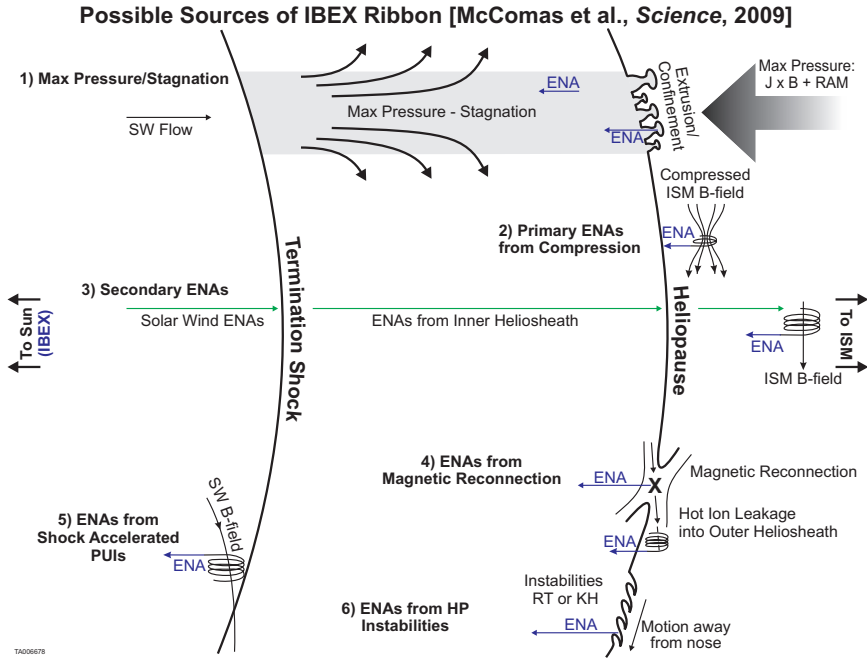


Fig. 6 Different possible sources of the enhanced ENA emission that forms the IBEX Ribbon are summarized in this cartoon. Possibility (1) generates ENA production in the regions of high pressure and plasma stagnation in the inner heliosheath, and possibly associated with heliopause distortions that create outward extrusions of plasma. Process (2) corresponds to ENAs produced preferentially with 90° pitch angles in the interstellar magnetic field that is compressed against the heliopause. The Lorentz force then provides the mechanism for diverting the particle momentum back to the inner heliosphere to be collected by IBEX. The third mechanism (3) creates secondary ENAs, in the inner heliosheath or inside the termination shock, through ionization and subsequent remission of outward traveling ENAs created from the solar wind and pickup ions. (4) The ENAs created from magnetic reconnection across the heliopause, which mixes inner heliosheath ions with neutrals, will show the direct imprint of the ISMF. (5) ENAs may be produced from shock accelerated ions close to the termination shock in the upstream and downstream regions. Possibility (6) produces ENAs in transient regions at the heliopause resulting from Rayleigh-Taylor or Kelvin-Helmholtz instabilities. This figure is from McComas et al. 2010.

Several possible mechanisms have been suggested for the formation of the Ribbon (McComas et al. 2009a, 2010). Figure 6 (McComas et al. 2010) illustrates possible scenarios suggested initially by the IBEX team.

(1) The Ribbon forms in inner heliosheath regions of maximum pressure, so that plasma flows away from the Ribbon (consistent with Voyager data) and the plasma stagnates. The pattern of ISM pressure (dynamic and magnetic) would imprint on the subsonic inner heliosheath, and those heliosheath regions with higher densities would emit more ENAs. Outwards extrusions, through the heliopause, of pockets of higher density gas might generate similar ENA spectra as the inner heliosheath. Schwadron et al. (2009) and Fuselier et al. (2009b) estimate a heliosheath thickness of $L \sim 50$ AU if the observed width and thickness

of the Ribbon are comparable. Hsieh et al. (2010) calculate ENA production from 0.04–4 MeV ions in the heliosheath measured by Voyager 1 and Voyager 2, and obtained a thicker Ribbon in the southern ecliptic hemisphere, $L = 28 \pm 8$ AU, than in the northern hemisphere, $L = 21 \pm 6$ AU, from comparisons with ENA data up to 0.1 MeV from SOHO/HSTOF. The larger heliosheath thickness inferred from the 44 keV *Cassini/INCA* (Krimigis et al. 2009) data may point to a more distant source region for these high energy ENAs. If the ring of higher interstellar pressure associated with the Ribbon is then felt inside of the heliopause, the large scale pressure driving the Ribbon is an external effect, and so would be expected to result in a largely stable feature (McComas et al. 2010).

(2) The Ribbon forms in outer heliosheath regions, possible from secondary ENAs (see (3)), where the ISMF is compressed against the heliopause. For this scenario, solar cycle variations should have less impact on the Ribbon than for (1). Three characteristics stand out for a Ribbon configuration originating beyond the heliopause, based on the MHD heliosphere model used in Schwadron et al. (2009, from Pogorelov et al., 2009). (a) The width of the Ribbon is controlled by the limits set on $|B \cdot R|$. (b) The length of the Ribbon arc is set by the limits set on total magnetic pressure, $\sim B^2$. (c) The latitude of the Ribbon arc, compared to the magnetic pole defined by the center of the arc, depends on the distance beyond the heliosphere of the Ribbon formation, so that a more distant ENA source location will slide the Ribbon towards the equator of the ISMF traced by the Ribbon arc.

(3) The third possible mechanism forms the Ribbon beyond the heliopause from secondary ENAs. Primary ENAs are produced from neutral charge-exchange with solar wind or inner heliosheath pickup ions, and propagate outwards past the heliopause where they convert back to energetic ions through charge exchange. These ions convert, via charge-exchange, to the secondary ENAs that propagate inwards to IBEX (Heerikhuisen et al. 2010; Florinski et al. 2010; Chalov et al. 2010). The mean free path of a 100 (400) km s^{-1} ENA in the outer heliosheath is ~ 250 (400) AU, suggesting that Ribbon ENAs must form over lengths of ≥ 200 AU. The long times (decade) for parent ions to travel outwards and return as ENAs might be expected to smooth out solar cycle variations and small scale structures in the ENA fluxes.

(4) ENAs from magnetic reconnection at the heliopause: Magnetic reconnection is a mechanism that directly mixes the interstellar and subsonic solar plasmas, and might form transient structures in the Ribbon in the regions where the interstellar pressure is at a maximum. Alternating solar polarities would disperse the reconnection across both hemispheres of the heliosphere, but a continuous Ribbon structure would need explaining.

(5) If the subsonic solar plasma disperses the increased interstellar pressure throughout the inner heliosheath, the termination shock location may also be affected, and therefore, the production or energization of pickup ions at the termination shock may increase.

(6) The dense interstellar plasma and tenuous time-variable solar wind plasma are separated by the tangential discontinuity known as the heliopause. The heliopause is generally thought to be unstable, either from shear instabilities or the effective gravity of charge-exchange (e.g. Dasgupta et al. 2006). Rayleigh-Taylor instabilities are expected to dominate near the heliosphere nose, and shear (Kelvin-Helmholz) instabilities near the heliosphere flanks. These instabilities directly mix the inner heliosheath solar wind and pickup ion plasmas with the interstellar neutrals and plasmas, and thereby could increase the ENA production rate (e.g. by reducing hydrogen filtration).

There is also at least one entirely new origin suggested for the Ribbon, whereby it is a viewpoint perspective of ENAs formed where ISNs in the interface on the circum-heliospheric interstellar gas charge-exchange with the surrounding hot plasma, $\sim 10^6$ K (Grzedzielski et al. 2010). Despite the strong agreement of the Ribbon location with the

MHD models that reproduce the draping of the ISMF over the heliosphere, the same field will affect the cloud around the Sun where it may create an analogous yet-unknown asymmetry.

5 Closing Comments

IBEX continues to return new ENA data that monitor the interaction between the solar wind and interstellar medium at the heliosphere boundaries. Two full sky maps have been completed and initially analyzed, and they show firmly that the fluxes of ENAs formed at the heliosphere boundaries vary with the solar magnetic activity cycle (McComas et al. 2010). The potential for ENAs to trace the relation between stellar winds and interstellar gas is enormous, with implications for the structure of the heliosphere and astrospheres around exoplanetary systems. IBEX is also expected to detect the solar transition between interstellar clouds if it occurs 'soon' (Frisch et al. 2010a). As data builds up over time on the population of interstellar neutrals that are detected by IBEX-Lo, such as hydrogen, helium and oxygen, the ability to develop self-consistent models of the physical properties of the ISM will also improve. IBEX data bridges the gap between solar system and Milky Way Galaxy by mapping the energetic neutral atoms that form from charge-exchange between interstellar neutral hydrogen atoms and the solar wind and pickup ions, and direct measurements of interstellar neutrals (Frisch et al. 2010a).

Acknowledgements We thank the IBEX team members for the exciting discoveries of the IBEX mission, and the International Space Sciences Institute in Bern, Switzerland, for hosting the workshop 'Galactic Cosmic Rays in the Heliosphere' where this review was presented. This work was funded through the IBEX mission, as a part of NASA's Explorer Program.

References

- T.F. Adams, P.C. Frisch, High-resolution observations of the Lyman alpha sky background. *ApJ* **212**, 300–308 (1977)
- J.L. Bertaux, J.E. Blamont, Evidence for a Source of an Extraterrestrial Hydrogen Lyman-alpha Emission. *A&A* **11**, 200 (1971)
- S.V. Chalov, D.B. Alexashov, D. McComas, V.V. Izmodenov, Y.G. Malama, N. Schwadron, Scatter-free Pickup Ions beyond the Heliopause as a Model for the Interstellar Boundary Explorer Ribbon. *ApJ* **716**, 99–102 (2010)
- B. Dasgupta, V. Florinski, J. Heerikhuisen, G.P. Zank, MHD Instabilities at the Heliopause, in *Physics of the Inner Heliosheath*, ed. by J. Heerikhuisen, V. Florinski, G. P. Zank, & N. V. Pogorelov . American Institute of Physics Conference Series, vol. 858, 2006, pp. 51–57
- V. Florinski, G.P. Zank, J. Heerikhuisen, Q. Hu, I. Khazanov, Stability of a Pickup Ion Ring-beam Population in the Outer Heliosheath: Implications for the IBEX Ribbon. *ApJ* **719**, 1097–1103 (2010)
- P.C. Frisch, The S1 Shell and Interstellar Magnetic Field and Gas Near the Heliosphere. *ApJ* **714**, 1679–1688 (2010)
- P.C. Frisch, J. Heerikhuisen, N.V. Pogorelov, B. DeMajistre, G.B. Crew, H.O. Funsten, P.H. Janzen, D.J. McComas, E. Möbius, H.R. Mueller, D.B. Reisenfeld, J.D. Schwadron, N. A. Slavin, G.P. Zank, Can IBEX Identify Variations in the Galactic Environment of the Sun using Energetic Neutral Atom (ENAs)? *ApJ* **719**, 1984–1992 (2010a)
- P.C. Frisch, B. Andersson, A. Berdyugin, H.O. Funsten, M. Magalhaes, D.J. McComas, V. Piirola, N.A. Schwadron, J.D. Slavin, S.J. Wiktorowicz, Comparisons of the Interstellar Magnetic Field Directions obtained from the IBEX Ribbon and Interstellar Polarizations. *ApJ* **724**, 1473–1479 (2010b)
- H.O. Funsten, F. Allegrini, G.B. Crew, R. DeMajistre, P.C. Frisch, S.A. Fuselier, M. Gruntman, P. Janzen, D.J. McComas, E. Möbius, B. Randol, D.B. Reisenfeld, E.C. Roelof, N.A. Schwadron, Structures and Spectral Variations of the Outer Heliosphere in IBEX Energetic Neutral Atom Maps. *Science* **326**, 964 (2009a)

- H.O. Funsten, F. Allegrini, P. Bochsler, G. Dunn, S. Ellis, D. Everett, M.J. Fagan, S.A. Fuselier, M. Granoff, M. Gruntman, A.A. Guthrie, J. Hanley, R.W. Harper, D. Heirtzler, P. Janzen, K.H. Kihara, B. King, H. Kucharek, M.P. Manzo, M. Maple, K. Mashburn, D.J. McComas, E. Moebius, J. Nolin, D. Piazza, S. Pope, D.B. Reisenfeld, B. Rodriguez, E.C. Roelof, L. Saul, S. Turco, P. Valek, S. Weidner, P. Wurz, S. Zaffke, The Interstellar Boundary Explorer High Energy (IBEX-Hi) Neutral Atom Imager. *Space Science Reviews* **146**, 75–103 (2009b)
- S.A. Fuselier, P. Bochsler, D. Chornay, G. Clark, G.B. Crew, G. Dunn, S. Ellis, T. Friedmann, H.O. Funsten, A.G. Ghielmetti, J. Googins, M.S. Granoff, J.W. Hamilton, J. Hanley, D. Heirtzler, E. Hertzberg, D. Isaac, B. King, U. Knauss, H. Kucharek, F. Kudirka, S. Livi, J. Lobell, S. Longworth, K. Mashburn, D.J. McComas, E. Möbius, A.S. Moore, T.E. Moore, R.J. Nemanich, J. Nolin, M. O'Neal, D. Piazza, L. Peterson, S.E. Pope, P. Rosmarynowski, L.A. Saul, J.R. Scherrer, J.A. Scheer, C. Schlemm, N.A. Schwadron, C. Tillier, S. Turco, J. Tyler, M. Vosbury, M. Wieser, P. Wurz, S. Zaffke, The IBEX-Lo Sensor. *Space Science Reviews* **146**, 117–147 (2009a)
- S.A. Fuselier, F. Allegrini, H.O. Funsten, A.G. Ghielmetti, D. Heirtzler, H. Kucharek, O.W. Lennartsson, D.J. McComas, E. Möbius, T.E. Moore, S.M. Petrinec, L.A. Saul, J.A. Scheer, N. Schwadron, P. Wurz, Width and Variation of the ENA Flux Ribbon Observed by the Interstellar Boundary Explorer. *Science* **326**, 962 (2009b)
- M.A. Gruntman, A new technique for in situ measurement of the composition of neutral gas in interplanetary space. *Planet. Space Sci.* **41**, 307–319 (1993). doi:10.1016/0032-0633(93)90026-X
- S. Grzedzielski, M. Bzowski, A. Czechowski, H.O. Funsten, D.J. McComas, N.A. Schwadron, A Possible Generation Mechanism for the IBEX Ribbon from Outside the Heliosphere. *ApJ* **715**, 84–87 (2010)
- J. Heerikhuisen, N.V. Pogorelov, G.P. Zank, G.B. Crew, P.C. Frisch, H.O. Funsten, P.H. Janzen, D.J. McComas, D.B. Reisenfeld, N.A. Schwadron, Pick-Up Ions in the Outer Heliosheath: A Possible Mechanism for the Interstellar Boundary EXplorer Ribbon. *ApJ* **708**, 126–130 (2010)
- M. Hilchenbach, K.C. Hsieh, D. Hovestadt, B. Klecker, H. Gruenwaldt, P. Bochsler, F.M. Ipavich, A. Buergi, E. Moebius, F. Gliem, W.I. Axford, H. Balsiger, W. Bornemann, M.A. Coplan, A.B. Galvin, J. Geiss, G. Gloeckler, S. Hefti, D.L. Judge, R. Kallenbach, P. Laeverenz, M.A. Lee, S. Livi, G.G. Managadze, E. Marsch, M. Neugebauer, H.S. Ogawa, K. Reiche, M. Scholer, M.I. Verigin, B. Wilken, P. Wurz, Detection of 55–80 keV Hydrogen Atoms of Heliospheric Origin by CELIAS/HSTOF on SOHO. *ApJ* **503**, 916 (1998)
- K.C. Hsieh, M.A. Gruntman, Viewing the outer heliosphere in energetic neutral atoms. *Advances in Space Research* **13**, 131–139 (1993). doi:10.1016/0273-1177(93)90402-W
- K.C. Hsieh, J. Giacalone, A. Czechowski, M. Hilchenbach, S. Grzedzielski, J. Kota, Thickness of the Heliosheath, Return of the Pick-up Ions, and Voyager 1's Crossing the Heliopause. *ApJ* **718**, 185–188 (2010)
- S.M. Krimigis, D.G. Mitchell, E.C. Roelof, K.C. Hsieh, D.J. McComas, Imaging the Interaction of the Heliosphere with the Interstellar Medium from Saturn with Cassini. *Science* **326**, 971 (2009)
- W.S. Kurth, D.A. Gurnett, On the source location of low-frequency heliospheric radio emissions. *J. Geophys. Res.* **108**, 2–16 (2003)
- R. Lallemand, E. Quémerais, J.L. Bertaux, S. Ferron, D. Koutroumpa, R. Pellinen, Deflection of the Interstellar Neutral Hydrogen Flow Across the Heliospheric Interface. *Science* **307**, 1447–1449 (2005)
- B.G. Lindsay, R.F. Stebbings, Charge transfer cross sections for energetic neutral atom data analysis. *Journal of Geophysical Research (Space Physics)* **110**, 12213 (2005)
- D.J. McComas, F. Allegrini, P. Bochsler, M. Bzowski, E.R. Christian, G.B. Crew, R. DeMajistre, H. Fahr, H. Fichtner, P.C. Frisch, H.O. Funsten, S.A. Fuselier, G. Gloeckler, M. Gruntman, J. Heerikhuisen, V. Izmodenov, P. Janzen, P. Knappenberger, S. Krimigis, H. Kucharek, M. Lee, G. Livadiotis, S. Livi, R.J. MacDowall, D. Mitchell, E. Möbius, T. Moore, N.V. Pogorelov, D. Reisenfeld, E. Roelof, L. Saul, N.A. Schwadron, P.W. Valek, R. Vanderspek, P. Wurz, G.P. Zank, Global Observations of the Interstellar Interaction from the Interstellar Boundary Explorer (IBEX). *Science* **326**, 959 (2009a)
- D.J. McComas, F. Allegrini, P. Bochsler, M. Bzowski, M. Collier, H. Fahr, H. Fichtner, P. Frisch, H.O. Funsten, S.A. Fuselier, G. Gloeckler, M. Gruntman, V. Izmodenov, P. Knappenberger, M. Lee, S. Livi, D. Mitchell, E. Möbius, T. Moore, S. Pope, D. Reisenfeld, E. Roelof, J. Scherrer, N. Schwadron, R. Tyler, M. Wieser, M. Witte, P. Wurz, G. Zank, IBEX–Interstellar Boundary Explorer. *Space Science Reviews* **146**, 11–33 (2009b)
- D.J. McComas, M. Bzowski, P.C. Frisch, G.B. Crew, M.A. Dayeh, R. DeMajistre, H.O. Funsten, S.A. Fuselier, M. Gruntman, P. Janzen, M.A. Kubiak, G. Livadiotis, E. Möbius, D. Reisenfeld, N.A. Schwadron, "the evolving outer heliosphere: Large-scale stability and time variations observed by the interstellar boundary explorer". *JGR* **00**, (2010)
- E. Möbius, D. Hovestadt, B. Klecker, M. Scholer, G. Gloeckler, Direct observation of He(+) pick-up ions of Interstellar Origin in the Solar Wind. *Nature* **318**, 426–429 (1985)

-
- E. Möbius, M. Bzowski, S. Chalov, H. Fahr, G. Gloeckler, V. Izmodenov, R. Kallenbach, R. Lallement, D. McMullin, H. Noda, M. Oka, A. Pauluhn, J. Raymond, D. Ruciński, R. Skoug, T. Terasawa, W. Thompson, J. Vallerger, R. von Steiger, M. Witte, Synopsis of the interstellar He parameters from combined neutral gas, pickup ion and UV scattering observations and related consequences. *A&A* **426**, 897–907 (2004)
- E. Möbius, P. Bochsler, M. Bzowski, G.B. Crew, H.O. Funsten, S.A. Fuselier, A. Ghielmetti, D. Heirtzler, V.V. Izmodenov, M. Kubiak, H. Kucharek, M.A. Lee, T. Leonard, D.J. McComas, L. Petersen, L. Saul, J.A. Scheer, N. Schwadron, M. Witte, P. Wurz, Direct Observations of Interstellar H, He, and O by the Interstellar Boundary Explorer. *Science* **326**, 969 (2009)
- M. Opher, J.D. Richardson, G. Toth, T.I. Gombosi, Confronting Observations and Modeling: The Role of the Interstellar Magnetic Field in Voyager 1 and 2 Asymmetries. *Space Science Reviews* **143**, 43–55 (2009)
- N.V. Pogorelov, J. Heerikhuisen, J.J. Mitchell, I.H. Cairns, G.P. Zank, Heliospheric Asymmetries and 2–3 kHz Radio Emission Under Strong Interstellar Magnetic Field Conditions. *ApJ* **695**, 31–34 (2009)
- D. Ruciński, A.C. Cummings, G. Gloeckler, A.J. Lazarus, E. Möbius, M. Witte, Ionization Processes in the Heliosphere - Rates and Methods of their Determination. *Space Sci. Rev.* **78**, 73–84 (1996)
- N.A. Schwadron, M. Bzowski, G.B. Crew, M. Gruntman, H. Fahr, H. Fichtner, P.C. Frisch, H.O. Funsten, S. Fuselier, J. Heerikhuisen, V. Izmodenov, H. Kucharek, M. Lee, G. Livadiotis, D.J. McComas, E. Möbius, T. Moore, J. Mukherjee, N.V. Pogorelov, C. Prested, D. Reisenfeld, E. Roelof, G.P. Zank, Comparison of Interstellar Boundary Explorer Observations with 3D Global Heliospheric Models. *Science* **326**, 966 (2009)
- J.D. Slavin, P.C. Frisch, The boundary conditions of the heliosphere: photoionization models constrained by interstellar and in situ data. *A&A* **491**, 53–68 (2008)
- G.E. Thomas, R.F. Krassa, OGO 5 Measurements of the Lyman Alpha Sky Background. *A&A* **11**, 218 (1971)
- V.M. Vasyliunas, A Survey of Low-Energy Electrons in the Evening Sector of the Magnetosphere with OGO 1 and OGO 3. *J. Geophys. Res.* **73**, 2839 (1968)
- C.S. Weller, R.R. Meier, Observations of helium in the interplanetary/interstellar wind - the solar-wake effect. *ApJ* **193**, 471–476 (1974)